A Numerical Assessment of an Effective Envelope-Tracking Semiconductor Optical Amplifier Design for Coherent-Optical OFDM Transmission

Julio Cesar Ortiz-Cornejo, Pascal Morel, Stéphane Azou, Jorge Arturo Pardiñas-Mir

A Numerical Assessment of an Effective Envelope-Tracking Semiconductor Optical Amplifier Design for Coherent-Optical OFDM Transmission

Julio Cesar Ortiz-Cornejo[1,2], Pascal Morel[3], Stéphane Azou[3], Jorge Arturo Pardiñas-Mir[1]

December 3, 2019

[1]ITESO, Guadalajara, Mexico
[2]Technological University of Jalisco, Mexico
[3]ENIB; CNRS, UMR 6285 Lab-STICC ; Brest, France

Abstract

The inherent nonlinear effects associated to Semiconductor Optical Amplifiers (SOAs) may translate into a transmission performance loss for non-constant envelope modulation formats. However, a variety of linearization schemes may be adopted for coping with these impairments and offering an effective system design. In this paper, an envelope tracking (ET) technique is investigated for linearizing an SOA-based Coherent Optical OFDM transmitter. An optimized design of the ET subsystem is performed under various scenarios, with the eventual joint use of Peak-to-Average Power Ratio (PAPR) reduction either via hard-clipping or nonlinear companding. A thorough carrier density analysis is performed in the amplifier, for various target gain values, so as to assess the effectiveness of the proposed scheme. Morever, we investigate the robustness of the proposed approach against some parameters variation both inside the ET path (DAC characteristics and bandwidth limited envelope generation). Extensive simulations performed with a precise SOA model show that up to 8 dB (resp. 7 dB) BER improvement can be achieved via the proposed scheme in the case of 4-QAM/OFDM (resp. 16-QAM/OFDM), compared to the conventional system with no linearization, and that even an envelope quantized with 2 bits still enables a significant performance increase.

1 Introduction

Multicarrier modulations [1, 2] have proved to be promising for satisfying the ever increasing capacity demand in optical fiber networks [3], with key features including high spectral efficiency, robustness to fiber chromatic dispersion and polarization mode dispersion, and powerful digital signal processing (DSP)-based implementation. However, multicarrier signals usually have the drawback of a non-constant enveloppe with possible large PAPR [4], which make them highly sensitive to the nonlinear distorsions.

The optoelectronics devices involved in fiber-optic communication systems may induce various specific nonlinear impairments, mainly at the transmitter side due to the sinusoidal characteristic of the optical modulator [5][6] or in the fiber due to the Kerr-effect at high launch power [7][8]. Further nonlinearities may be caused by optical amplifiers, specially if SOAs are adopted [12]. With the use of spectrally efficient modulation formats these nonlinear impairments can translate into serious performance degradation and their compensation via digital signal processing techniques is the subject of a growing literature. Popular techniques encompass digital predistortion, digital back-propagation, volterra series based nonlinear equalization or machine learning.

In this manuscript, we focus on the nonlinear effects associated to SOA used as a booster amplifier. As pointed out in a number of recent studies [10][11][12], SOA may be an alternative to the reference Erbium-Doped Fiber Amplifier (EDFA) technology in future WDM optical networks, due to their interesting key features including low-cost, wide optical bandwidth, compactness and integrability. However, in some scenarios, compensation techniques appear to be of critical importance for combating the intrinsic nonlinear gain dynamics of the SOA and thus achieving favorable system performance. Different techniques have been reported so far, with various cases depending on the role of the SOA (booster, in-line amplifier

or pre-amplifier, with possible cascade) and on the number of channels involved. Some techniques alleviate the nonlinear distortions via digital signal processing like digital backpropagation [13][14] or digital predistortion [15][16], and non-DSP schemes have also been investigated, like feedforward linearization [17], gain-clamped SOA [18] and non-uniform biasing [20, 19]. Other efforts have focused on changing the device design, either with multi-contact SOA [21] or Quantum-Dot structure [22].

In this manuscript, we investigate the design of an ET sub-system for coping with SOA nonlinear impairments, the amplifier being used as a power booster in a CO-OFDM system. This study is in the continuity of some of our previous works, including [23] in which we pointed out the effectiveness of ET-SOA for amplifying multicarrier signals and [24] devoted to the optimal tuning of some parameters of the ET block jointly with PAPR reduction, with the view to minimize the Error Vector Magnitude (EVM) [25]. A few other studies are identified in the literature regarding bias current control of SOAs for improving the transmission performance. These prior contributions share some similarities with our work, even if they have different objectives and system setups. Saleh et al. [19] have shown for the first time that varying the bias current may theoretically lead a constant average carrier density in the SOA while amplifying non-constant envelope signals. The authors conducted an experiment for showing the linearization performance with a two-tone signal at input of the SOA, which is used as an inline amplifier. Around 14 dB reduction in the intermodulation distortion over a wide range of input power has been reported in this work, for a frequency separation going up to 1.25 GHz between the two tones. Later, Ng et al. [20] proposed an optimized non-uniform bias current so as to achieve SOA gain uniformity in presence of high speed input pulses. In a recent work, Fujiwara and Koma [26] proposed to vary the SOA bias current to cope with the near-far problem typical of PON upstream transmission. The approach relies on a cascade setup with use of a fast feedforward control circuit applied to the first SOA and output burst frame powers being equalized in the second SOA. More recently, Dalla Santa et al. [27] have investigated an SOA bias current control strategy for optical equalization of the upstream in a PON system with four 25Gb/s channels and multilevel modulation format, the SOA being used as a pre-amplifier. Such adaptive biasing schemes actually shares some similarities with the popular envelope tracking (ET) technique [28][29] used for inscreasing RF power amplifier efficiency, by modulating the supply voltage according to the input signal envelope fluctuation. Compared to digital baseband predistortion techniques, an ET scheme for linearizing SOA offers the advantage that it can be applied with a very similar approach whether SOA is used as a booster or as inline amplifier, with no strict requirement regarding the linearizer tuning (no learning stage). In addition, ET may offer a larger performance gain. Many extensions are proposed in this manuscript to corroborate the capability of ET for achieving highly linear coherent optical transmitters including an SOA. First, the carrier density through SOA active region is examined under an ET regime. Second, an optimization of the ET-subsystem is reported for various scenarios with an eventual joint use of hard clipping or soft clipping, considering various SOA target gains and QAM modulation orders. Third, the robustness of the optimized ET-SOA-based CO-OFDM transmitter is studied for changes of some parameters of the ET sub-system (low-pass filter bandwidth; DAC sampling rate and resolution) or in presence of some laser wavelength shift.

Even if we consider a conventional CP-OFDM modulation format [30] in this manuscript, our study is actually general and we think that it may be of interest for other researchers interested in the use of SOAs with any other advanced non-constant envelope modulation format offering higher spectral efficiency , like OFDM/OQAM [2]. Also, we consider PAPR reduction via nonlinear companding, but our objective is to reveal that combining ET with PAPR reduction translates into a significant transmission performance gain and this conclusion also holds if another PAPR reduction technique is used.

The rest of this paper is organized as follows. Section 2 briefly reminds the relation between the SOA's optical gain and its bias current, and describes our Envelope Tracking SOA System Model. Then, in section 3, the carrier density is analyzed under an envelope tracking regime. Section 4 deals with the ET block optimization and reports the performance inscrease compared to a system without linearization. Then, section 5 investigates the robustness of the proposed ET-SOA-based CO-OFDM transmitter to some parameters changes. Finally, some important conclusions are drawn.

2 Semiconductor Optical Amplifier Linearization by Envelope Tracking

2.1 Controlling SOA dynamics via non-uniform bias current

SOA is a multipurpose device that can not only compensate for fiber losses but also enable the all-optical implementation of many functions (such as regeneration, switching or wavelength conversion) required in

modern optical networks [31]. If the inherent device nonlinearity is very useful in the latter case, it turns out to be a major drawback when it comes to handling the power budget with non-constant envelope signals. Nevertheless, it has been pointed out in a number of studies that SOAs may be a pertinent choice for amplifying advanced modulation formats [11]. For OFDM signals, use of some linearization schemes have been recommended so as to cope with the large PAPR typical of such format [32].

SOA gain saturation is actually likely to introduce signal distortions translating into transmission quality degradation. To alleviate these distortions a high saturation output power is required. SOA's optical gain is defined as a function of the carrier density N by

$$G = \exp\left[\Gamma a \left(N - N_t\right) L\right] \tag{1}$$

where L denotes the SOA length, Γ is the confinement factor, a is the differential gain and N_t is the carrier density at transparency [31]. The gain results from the effect of population inversion inside the active region, under the influence of the set bias current. The population inversion may be reduced in situations where the injected optical signal exhibits occasional high peaks; then, a carrier density depletion may occur near the output section, as a result of large photon density, which translates into nonlinear impairments. Thus, SOA's optical gain is mainly controlled by the carrier density generation. We consider the following classical rate equation for the carrier density N, with only one SOA section,

$$\frac{dN}{dt} = \frac{I}{qV} - \frac{N}{\tau} - \frac{(G-1)P_{\text{in}}}{h\nu V} \tag{2}$$

where I stands for the injected electrical current, q corresponds to the elementary charge, V is the active zone volume, h is Planck's constant, ν the frequency of light, and τ denotes the carrier lifetime.

In the small-signal regime, and neglecting the second-order terms, it can be shown that the following model holds for the carrier density dynamics in a single section SOA [24], if a non-uniform bias current $i(t) = (G_0 - 1)\frac{p(t)q}{h\nu}$ is adopted,

$$n(t) \sim \exp\left[-\frac{t}{\tau}\left(1 + \frac{G_0 P_0}{P_{\text{sat}}}\right)\right] \tag{3}$$

where G_0 and P_0 are SOA gain and input power, respectively, and P_{sat} corresponds to the material saturation power.

The above expression means that if a proper dynamic bias current is applied to the device, $\lim_{t\to\infty} n(t) = 0$ and the carrier density tends to be constant, meaning a linear behavior of the SOA. In the following subsection, we describe a setup based on an envelope tracking scheme with the view to maintain a constant carrier density in an SOA used for boosting the power of multicarrier signals at the transmitter.

2.2 Envelope Tracking SOA System Model

Envelope tracking consists in dynamically adjusting the SOA bias current proportionally to the incoming optical signal's envelope with the view to maintain the carrier density at a constant value. The ET-SOA system under study, depicted in Fig. 1, corresponds to a CO-OFDM transmitter embedding an SOA as a power booster. In the present manuscript, extended results are derived with respect to our previous contributions [23, 24] which considered a similar setup. The baseband multicarrier signal is generated according to a standard CP-OFDM format and a companding transform is then eventually applied so as to reduce the PAPR [4]. Nonlinear companding aims at changing the amplitude statistics via a function $f(.)$ which has to be inverted at the receiver side for recovering the original signal plus noise. In this study, we consider again the μ-law scheme, which can achieve a good complexity/performance tradeoff [33] with only one parameter,

$$y[n] = f(x[n]) = \text{sgn}(x[n])\frac{A}{\ln(1+\mu)}\ln\left(1 + \frac{\mu}{A}|x[n]|\right) \tag{4}$$

where $sgn(.)$ stands for the complex *signum* function, A is the maximum amplitude of the baseband signal $x[n]$, $\mu > 0$ is the companding parameter and $|x[n]|$ denotes the amplitude of $x[n]$.

In addition to this technique, a hard-clipping scheme will also be considered for comparison purposes. Despite its simplicity and the induced in-band and out-of-band distortions, it has been pointed out that this approach may lead to favorable performance tradeoff [6].

The resulting signal $y[n]$ is fed into the envelope tracking path and in parallel, after some delay adjustment and digital-to-analog conversion, is injected into the IQ optical modulator which has a half-wave voltage V_π of 6 V and a 1540 nm continuous-wave light applied at its input. The obtained optical signal is finally boosted by an SOA which operates under envelope tracking regime and the performance is evaluated in a back-to-back configuration (the amplified signal is directly sent to the receiver). At the receiver side, no frequency equalization is performed.

In our study, a self-developed SOA model, which has been fitted to simulate a commercially available bulk 750 μm long SOA (INPHENIX-IPSAD1501), is considered. This model, originally developed in [34], has proved to be highly effective in various problems, including all-optical RF mixer design based on cross-gain modulation in a SOA [35], coherent optical OFDM signal amplification via SOA [9] or RSOA-based IM/DD OFDM transmission [36]. More specifically, in the latter work, the intensity modulation of the CW optical signal from the laser source is achieved by varying the amplifier current with the OFDM signal to be transmitted (an adaptive format being eventually used depending on the transmission quality observed on the various subcarriers). Also, the XGM effect in the SOA is used for achieving a wavelength conversion for the IM-OFDM signal. A comparison between numerical results and measurements is also conducted. Overall, a good agreement is noticed which reveals that our SOA model can realistically reflect the amplifier behavior under high speed bias current variation.

In the ET path, the envelope $e[n] = |y[n]|$ of the RF baseband complex signal is first low pass filtered using a FIR filter so as to alleviate the implementation complexity for the following DAC.

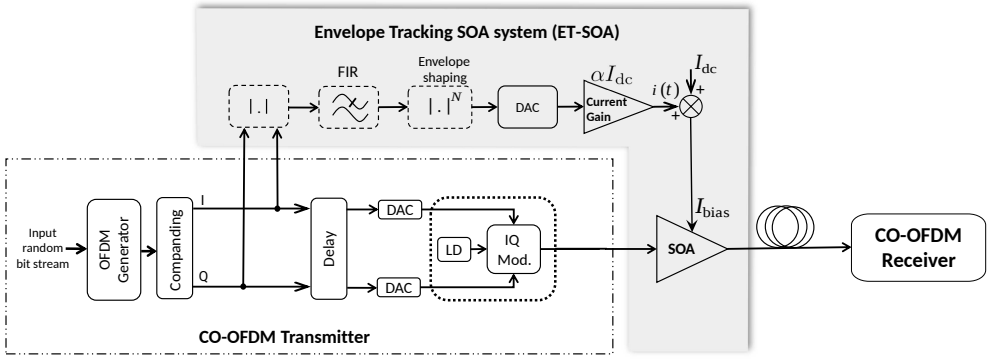

Figure 1: The considered CO-OFDM transmitter scheme, embedding an ET-SOA for boosting the signal power.

A nonlinear shaping function (NLSF) of the form $|e_f[n]|^N$ is then applied to the filtered envelope $e_f[n]$ with the view to take advantage of the degree of freedom N for improving the linearization efficiency. For $N > 1$ the NLSF compresses the low amplitudes and increases the highest ones, leading to a larger bias current when SOA needs to increase the carrier density to counteract the carrier density depletion. Note that from the analysis given in previous subsection, $N = 2$ is expected to give the best performance, as also pointed out in other references [19].

The shaped envelope signal $e_s(t)$ obtained from the DAC is scaled so that the bias current is adapted as

$$I_{\text{bias}}(t) = I_{\text{dc}} + i(t) \tag{5}$$

with

$$i(t) \simeq \alpha I_{\text{dc}} |e_f(t)|^N \tag{6}$$

where α denotes the gain used for scaling the dynamic part of the current and $e_f(t)$ is the bandwidth limited envelope corresponding to the baseband signal $y[n]$.

3 Carrier Density Analysis under Envelope Tracking Regime

As mentioned in the previous section, carrier density governs the SOA gain. In this section the carrier density through SOA active region is investigated, and the benefits of envelope traking for carrier density depletion reduction is shown for an optimal tuning of the ET block (in the case where the shaping function uses $N = 2$) combined with μ-law companding.

3.1 Numerical simulation

To carry out the numerical simulations, SOA active region has been divided into 8 sections to compute the carrier population inversion which is responsible for the optical amplification process. Simulations were conducted for a frame made of 2^{11} 4-QAM symbols with 128 subcarriers, occupying a bandwidth of 5 GHz to be consistent with our previous studies [23, 24]. Later in the article, a larger bandwidth of 20 GHz will be considered while keeping the same subcarrier spacing (use of 512 subcarriers). Note also that throughout this study the QAM symbols are mapped onto the whole set of subcarriers.

Each performed simulation results in a matrix $\boldsymbol{N} = [N_{lm}] \in \mathbb{R}^{L \times M}$ reflecting the carrier density variation along the SOA's M sections for the l-th injected signal sample ($l = 1, 2, ..., L$). A fine analysis of the carrier density dynamics can then be conducted in presence of multicarrier signals, and the effectiveness of some linearization schemes can then be assessed from the device inherent properties.

Two cases have been considered for an SOA operating in saturation with an injected optical power of -7 dBm and 15 dB of gain: the first one corresponds to a classical CO-OFDM transmission, with no linearization nor PAPR reduction, yielding an EVM performance[1] of 78 %. In a second case an optimal tuning of the ET-SOA system is adopted with joint use of μ-law companding, resulting in a far better performance with 20% EVM.

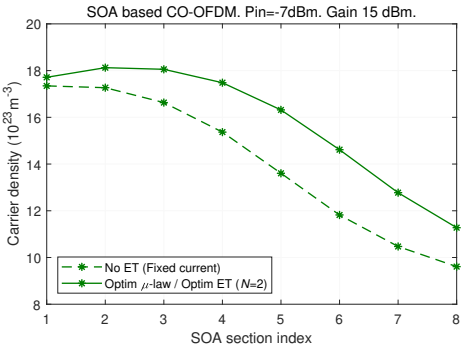

Figure 2: Carrier density variation for one signal sample passing through the SOA active region, for a conventional CO-OFDM transmitter employing SOA as a booster with constant bias current and for an envelope tracking-based transmitter.

Fig. 2 illustrates the carrier density change when one CO-OFDM sample is passing through the SOA active region. If the SOA is driven by a constant bias current, a large decrease of the carrier density can be observed, especially from the third SOA section. This effect is because a signal with higher power will interact with a larger number of excited electrons in the conduction band, thus resulting in depletion of carrier density and SOA gain. In contrast, a non-uniform bias current via envelope tracking enables a significant reduction of this issue.

Likewise, Fig. 3 shows the carrier density variation along the device, as a surface response for 500 CO-OFDM samples injected. The first subplot (a) corresponds to the classical implementation using a fixed bias current. A similar behavior as before can be observed, with an almost constant carrier density around $17{,}1.10^{23}\text{m}^{-3}$ at the input, followed by a slight increase up to $18{,}61.10^{23}\text{m}^{-3}$ over the next two sections and finally a large carrier depletion beyond the fourth section with a density falling around $9{,}32.10^{23}\text{m}^{-3}$. In the second subplot (b), an optimally tuned ET-SOA implementation is adopted. It can be clearly seen that the device exhibits a totally different behavior, with less spread of the carrier density together with less imbalance between the input ($15{,}59.10^{23}\text{m}^{-3}$) and output ($11{,}08.10^{23}\text{m}^{-3}$) values.

A complementary comparative illustration is given in Fig. 4, with the sample distributions of the carrier density along the SOA active region, for a CO-OFDM frame of 2^{15} 4-QAM samples. A strong carrier depletion is revealed by subplot (a) corresponding to a constant bias current, whereas a more stable carrier density can be observed in the case of an ET-SOA scheme (subplot b).

3.2 Gain influence in an ET-SOA

We now consider the influence of increasing the SOA gain on the carrier density while achieving a non constant bias current via envelope tracking with a target gain in the range $[15, 21]$ dB. As before, the

[1]Throughout the manuscript, a normalization by the average constellation power is used for computing the EVM.

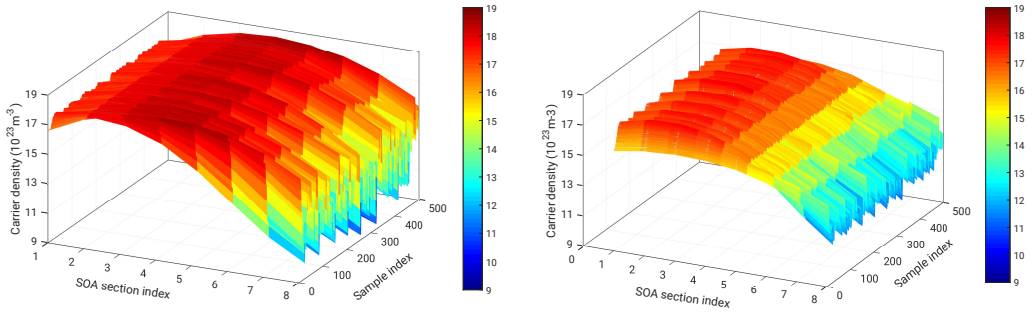

(a) (b)

Figure 3: Carrier density variation in the SOA for a CO-OFDM signal made of 500 samples; (a) constant bias current, (b) non uniform biasing via envelope tracking.

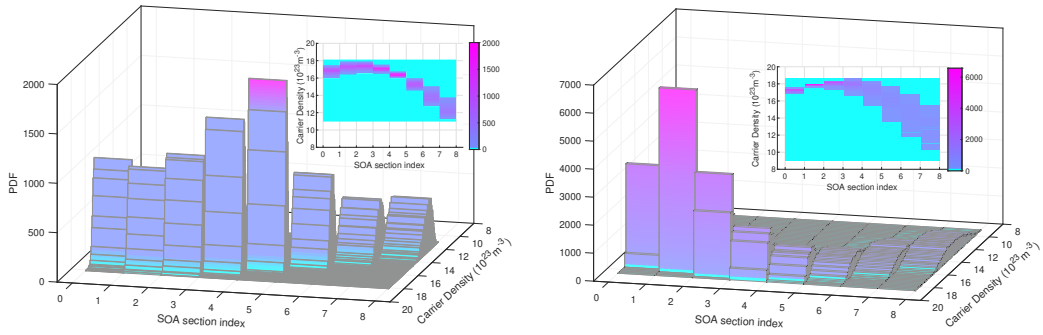

(a) (b)

Figure 4: Sample distribution of carrier density against the SOA section. (a) constant bias current, (b) non uniform biasing via envelope tracking.

ET subsystem still operates at its optimum tuning and with $N = 2$. For an injected optical power going from -19 dBm up to -5 dBm, we evaluated the minimum and the maximum carrier density in the active region. The results are depicted in Fig. 5. The first subplot shows the minimum value of the carrier density, which is observed at the ouput of the active region. It is first seen that going towards high input power translates into accentuated carrier depletion, as a result of more pronounced nonlinear effects. However, an interesting feature of the ET-SOA is that rather close values of the minimum carrier density are obtained despite an increased target gain. The next subplot illustrates the maximum carrier density recorded over the whole active region. Clearly, combating strong nonlinearities tends to require a higher bias current, which turns into a higher maximum carrier density value. Also, a neat difference can be noted between the curves revealing that boosting the gain translate into a huge increase of the peak carrier density. All these values were obtained by using an optimal design of ET-SOA system following the same optimization algorithm than in [24], but reoptimizing for new target gain values (in our previous work only the value 15 dB has been considered).

4 Optimization of the ET-SOA-based CO-OFDM transmitter

This section describes the optimization of the envelope tracking subsystem by eventually jointly using a clipping scheme for handling the PAPR, with the view to get the best EVM performance for the CO-OFDM system in a back-to-back setup. The same cost function $J(\boldsymbol{p})$ as in our previous work [24] is adopted, with extended scenarios and investigations,

$$J(\boldsymbol{p}) = \varepsilon \left| G(\boldsymbol{p}) - G^* \right| + EVM(\boldsymbol{p}) \ , \ \boldsymbol{p} \in \mathcal{D} \tag{7}$$

where $\boldsymbol{p} \in \mathcal{D}$ stands for the vector of parameters in the domain $\mathcal{D}$, $G(\boldsymbol{p})$ is the observed SOA gain in steady state, G^* denotes the target gain, $EVM(\boldsymbol{p})$ is the error vector magnitude and ε represents a weighting factor.

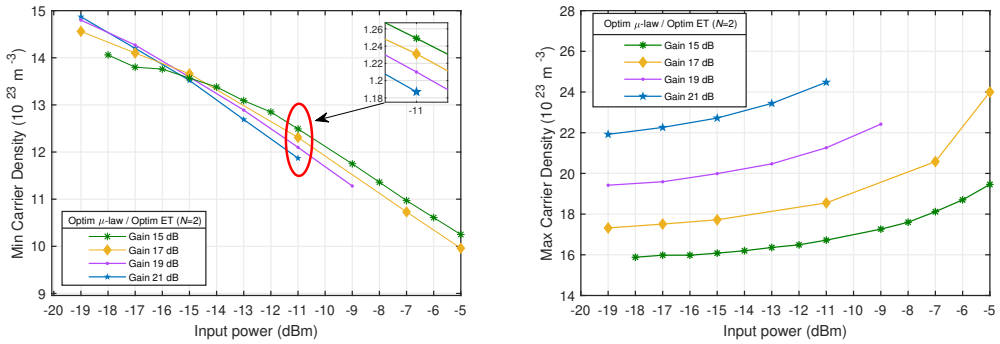

(a) (b)

Figure 5: Range of the carrier density in the SOA active region under envelope tracking optimal regime, for different target gain values and 2^{12}CO-OFDM signal samples. (a) Minimal carrier density (b) maximal carrier density.

Note that the parameters and the corresponding search space may depend on the considered scenario. In the present study, the following four cases have been investigated:

1. ET optimization with no PAPR reduction,

$$\boldsymbol{p} = [\alpha, I_{dc}, N]$$
$$\mathcal{D} = \{0.01 < \alpha < 2,\ 80\ \text{mA} < I_{dc} < 200\ \text{mA},\ 0.8 < N < 3\}$$

2. ET optimization with fixed μ-law nonlinear companding ($\mu = 2$),

$$\boldsymbol{p} = [\alpha, I_{dc}, N]$$
$$\mathcal{D} = \{0.01 < \alpha < 2,\ 80\ \text{mA} < I_{dc} < 200\ \text{mA},\ 0.8 < N < 3\}$$

3. Joint optimization of ET and μ-law nonlinear companding, with fixed envelope shaping ($N = 2$),

$$\boldsymbol{p} = [\alpha, I_{dc}, \mu]$$
$$\mathcal{D} = \{0.01 < \alpha < 2,\ 80\ \text{mA} < I_{dc} < 200\text{mA},\ 1 < \mu < 255\}$$

4. Joint optimization of ET and hard-clipping, with fixed envelope shaping ($N = 2$),

$$\boldsymbol{p} = [\alpha, I_{dc}, \gamma]$$
$$\mathcal{D} = \{0.01 < \alpha < 2,\ 80\ \text{mA} < I_{dc} < 200\text{mA},\ 1\,\text{dB} < \gamma < 12\,\text{dB}\}$$

where $\gamma = A'/E\{|x[n]|\}$ stands for the clipping ratio of the baseband OFDM signal $x[n]$, expressed in dB, and A' being the clipping threshold.

Heuristic optimization methods appear to be well suited to solving this nonlinear optimization problem, for their ability to perform derivative-free global optimization in presence of many parameters and constraints. In particular, we consider a Particle Swarm Optimization (PSO) scheme, which has proved to be highly effective in many engineering problems while being simple to implement [37]. The approach, first introduced in [38], consists in emulating a swarm behavior, where one group of individuals follows one of the members through a space looking for the best location. PSO algorithm produces an initial random population of particles where the cost function is evaluated. Then, the particles iteratively move towards the best location by adapting their speed and location until a stopping criterion is reached. In our study, the algorithm was set up with a swarm size of 80, and a stopping criterion of 20 stall generations or a minimum change of 10^{-3} for the objective function. The optimization is performed over the non-saturated and saturated regions of the SOA, with an input optical power ranging from -19 dBm up to -5 dBm.

As reported in our previous work [24], the third optimization scenario offers the best SOA linearization performance with a huge transmission quality improvement, as far as 8 dB power margin at a target

uncoded BER of 10^{-3} compared to the conventional system implementation (4-QAM/OFDM with no ET nor PAPR reduction), when the SOA operates at a gain of 15 dB. The optimization results are reported in Fig. 6, in terms of EVM with respect to input optical power. As can be observed, a large improvement is brougth by the nonlinear companding, as for scenario #1 a power penalty of around 5 dB is observed at 30% EVM, in comparison with scenario #3. On this plot we also report the complementary results for the fourth scenario including hard-clipping optimization. A significant EVM improvement can be seen in this case with respect to the conventional system, especially at high input power (enhancement of 2 dB at 30% EVM). We also consider on the same plot the approach described in [23] revisited with an SOA target gain of 15 dB; in this approach, a simple processing is achieved in the ET subsystem with use of the scaling gain α only, and a joint use of a μ-law companding in baseband with $\mu = 2$. If this scheme copes with slight nonlinear impairments, with performance very close to implementation #3 up to a power of -15 dBm, its effectiveness is rapidly decreasing as the operating point moves towards SOA saturation regime.

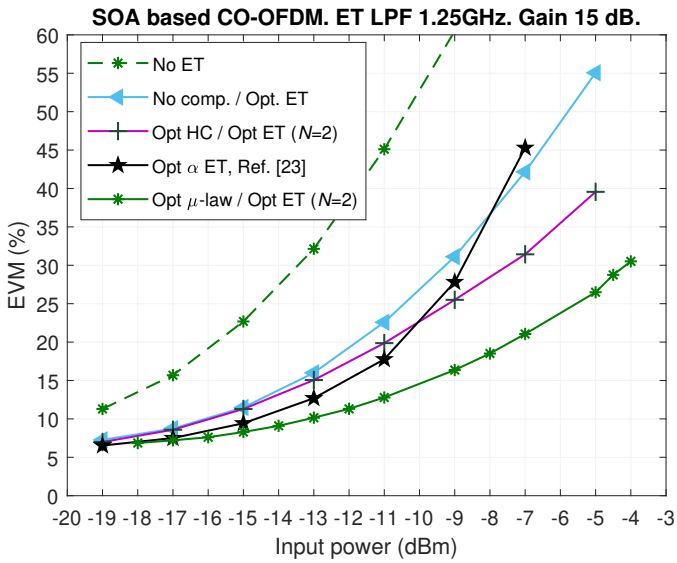

Figure 6: EVM as a function of input optical power for various system setups.

4.1 ET-SOA optimization for various SOA target gains

As shown by the previous simulations, the scheme #3 outperforms other implementations if the SOA operates at a gain of 15 dB. We now investigate the influence of the SOA target gain by considering larger values (17 dB, 19 dB, 21 dB), and therefore higher nonlinearities. For each input optical power and SOA gain, parameters (α, I_{dc}) in the ET block have been reoptimized (with a fixed envelope shaping, i.e. $N = 2$) jointly with the μ parameter of the nonlinear companding. The obtained results are depicted in Fig. 7, in comparison with the standard system operating with constant bias current. The proposed scheme offers a neat EVM improvement and even at a SOA gain of 21 dB the system still operates with a large performance advantage.

Likewise, the same optimization process has been conducted for a fixed input power of -13 dBm while increasing the SOA gain, still in comparison with standard implementation. As displayed by Fig. 8.a, investigating the relation between the gain and the required bias current, use of the proposed scheme tends to decrease the bias current on average. The second subplot (Fig. 8.b) exhibits a growing EVM enhancement thanks to optimized ET-SOA scheme as we move towards large SOA gain. The proposed technique still succeeds in linearizing the SOA at a gain of 25 dB, with an EVM less than 25%.

4.2 ET-SOA optimization for 16-QAM/OFDM format

Until now, only the 4-QAM/OFDM format has been considered in our work. Due to the SOA nonlinear effects, use of a higher modulation order makes the transmission more challenging while meeting a given quality of service. To extend our investigations we now examine the performance of our ET-SOA-based system in presence of 16-QAM/OFDM modulation format, still with the optimization setup #3 which

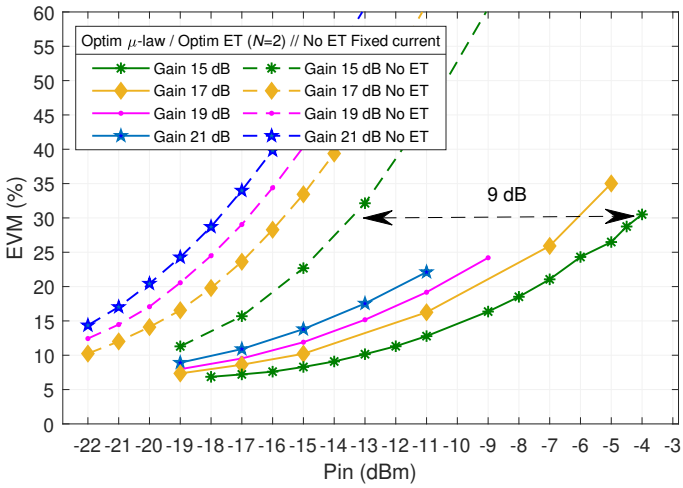

Figure 7: EVM as a function of input optical power using an optimized ET path (scenario #3), for different SOA gain values.

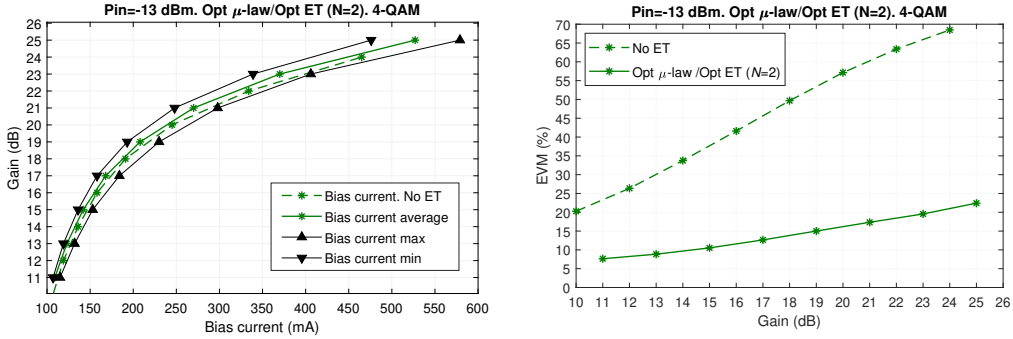

(a) (b)

Figure 8: Analysis of optimal ET-SOA in comparison with conventional SOA for an input optical power of -13 dBm. (a) Gain as a function of I_{dc} ; (b) EVM performance as a function of target gain.

appeared to be the best option in our previous analysis. The results are sketched in Fig. 9, in comparison with the 4-QAM/OFDM case. The EVM performance is reported in the first subplot. In absence of linearization, the 16-QAM/OFDM system has poor EVM performance. The theoretical limit of 13% EVM, which should not be exceeded if a 10^{-3} BER is desired [25], only allows to operate up to -19 dBm. By adopting the optimum ET-SOA tuning (scenario #3), it can be seen that a huge EVM improvement is gained with the possibility to operate up to a power of -12 dBm. The second subplot is devoted to the BER performance. Considering a target BER of 10^{-3}, an increase of around 7 dB of power at the SOA input can be achieved thanks to envelope tracking in the case of 16-QAM/OFDM format.

The system behavior is investigated in the frequency domain in Fig. 10. The first subplot reveals no significant distorsion induced by the amplifier, which is controlled by its ET block. In the second subplot, it can be observed that the average EVM per subcarrier has a relatively low spreading (it should be remembered that there is no use of frequency equalizer here).

5 Robustness analysis

Keeping the same tuning of the envelope tracking block while operating with different system settings is highly desirable in practice. In this section, we focus first on the influence of the lowpass filter cutoff frequency together with the DAC sampling rate and resolution while preserving the optimum settings of the ET-SOA subsystem (still with scenario #3); then we pursue by investigating the impact of any laser wavelength shift and finally the effect of increasing the bandwidth of the CO-OFDM signal is examined.

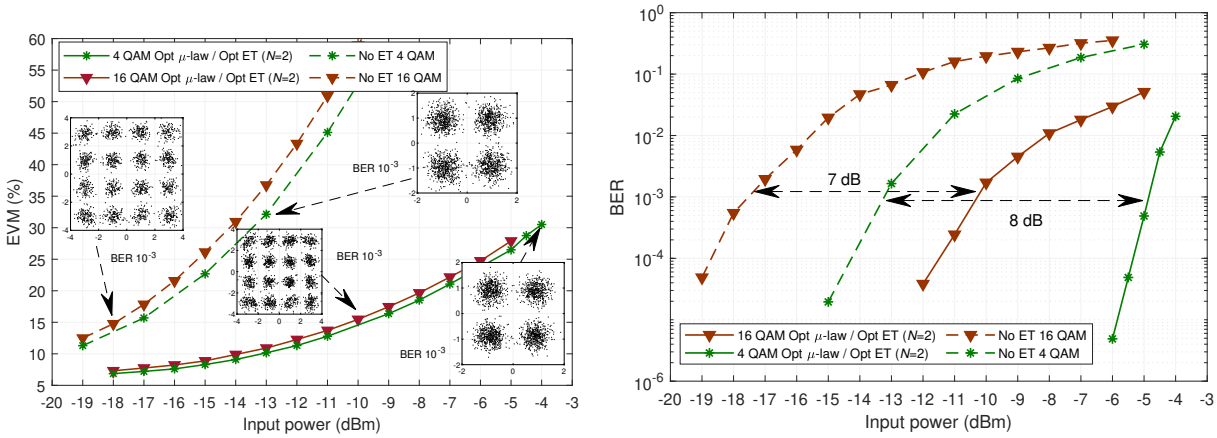

Figure 9: ET-SOA-based transmitter optimal performance with 4-QAM/OFDM and 16-QAM/OFDM modulation formats (use of optimization setup #3). (a) EVM performance (b) BER performance.

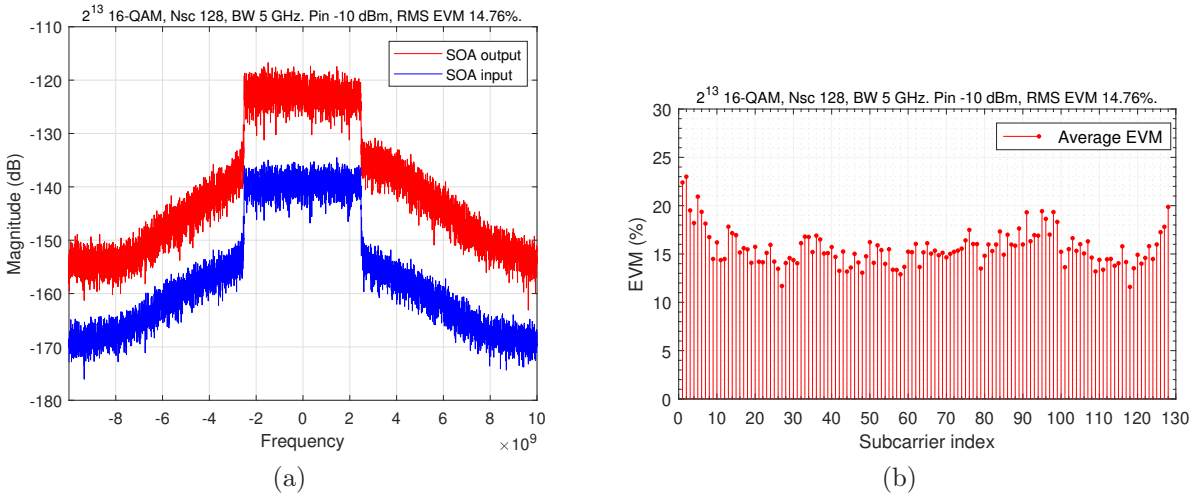

Figure 10: ET-SOA subsystem analyzed in the frequency domain (16-QAM case, Input power of -10 dBm); (a) Power spectral density of the signal at SOA input/output (b) Average EVM per subcarrier.

5.1 Filtering and Digital-to-Analog Converter influence

The results reported so far have been obtained using an infinite precision DAC. But for practical application, a low complexity of implementation must be assessed while maintaining an acceptable quality of service. So, the effectiveness of the ET-SOA scheme designed previously is now evaluated for various DAC sampling rates and resolutions while keeping the same optimal parameters as before (α, I_{dc}, μ, N). The considered DAC is based on a uniform quantization scheme, with input range correponding to the maximum/minimum signal amplitudes. In this study, the cutoff frequency of the lowpass filter used prior to the conversion will be also changed.

As illustrated in Fig. 11 the lowpass filter and the DAC strongly contribute to the envelope signal dynamics modification, specially in the considered example where a 2 bits DAC is used.

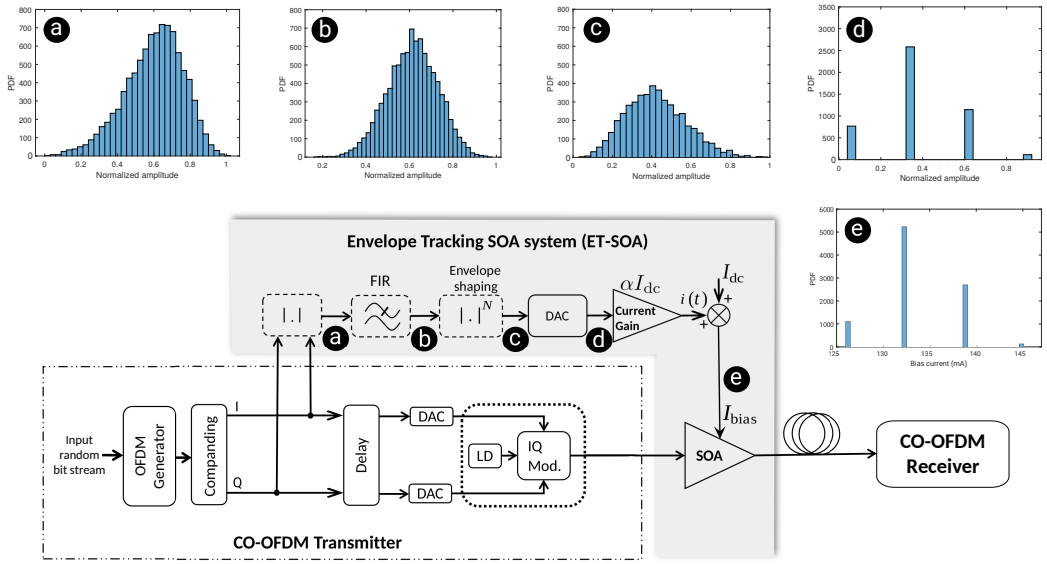

Figure 11: Block-diagram of the Envelope Tracking SOA-based CO-OFDM transmitter with an envelope filtered at 1.25 GHz and using a 2 bits Digital-to-Analog Converter (the original 4-QAM/OFDM signal has a bandwidth of 5 GHz and 128 subcarriers). The distribution of the signal amplitude is illustrated in various points of the ET block: (a) OFDM signal, being eventually companded (b) Bandwidth limited envelope (c) Nonlinearly shaped envelope ($N = 2$) (d) Quantized envelope (2 bits DAC) (e) Non-uniform bias current.

The EVM performance of the proposed ET-SOA-based CO-OFDM transmitter (tuned according to scenario #3 described in section 4, with 4-QAM/OFDM signal occupying a bandwidth of 5 GHz with 128 subcarriers) in presence of filter cutoff frequency, DAC sampling rate and resolution changes is studied in Fig. 12. Overall the system exhibits a good robustness to the parameters changes but it is clear that a very slow envelope, resulting from a filtering at 625 MHz, does not lead to suitable EVM performance. For the lowest complexity implementation (filter cutoff frequency at 625 MHz, sampling frequency of 1.25 GHz and 2 bits DAC), an EVM of 21 % is obtained. Increasing the sampling rate and the number of bits tends to lower EVM (as it is the case for all the filter bandwidth values) but the too slow envelope can not fullfill the objective of a constant carrier density in the SOA active region. A decent performance is observed once the filter bandwidth is above 1.25 GHz, provided that the DAC has at least 3 bits. Among the various combinations, a good complexity/performance tradeoff may be achieved for 1.88 GHz filter cutoff frequency. Fig. 13 gives a complementary insight into this setup, for a 10 GS/s sampling rate, with the variation of EVM against SOA input optical power, for various DAC resolutions.

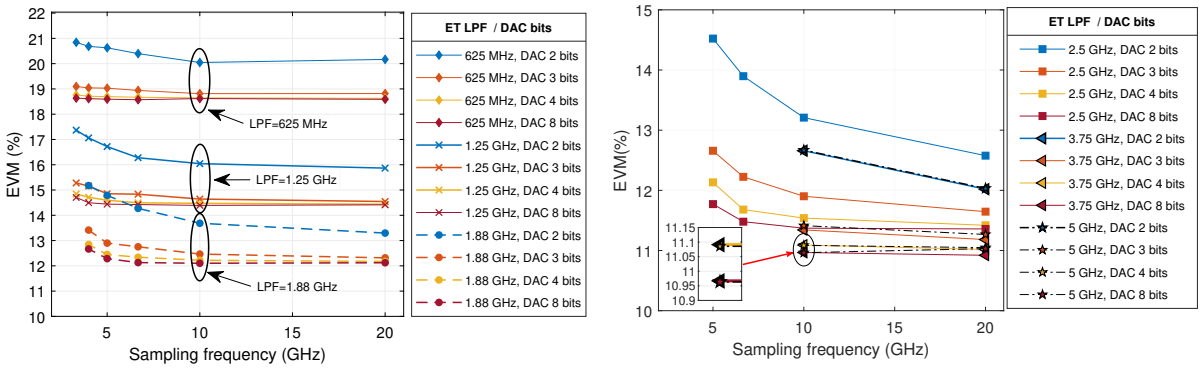

(a) (b)

Figure 12: Influence of some ET block parameters (lowpass filter cutoff frequency, DAC sampling rate and resolution) on the proposed ET-SOA-based CO-OFDM transmitter, operating with fixed $\{\alpha, I_{dc}, \mu, N\}$ specification resulting from PSO optimization (scenario #3). The SOA operates at a gain of 15 dB, with an input optical power of -10 dBm.

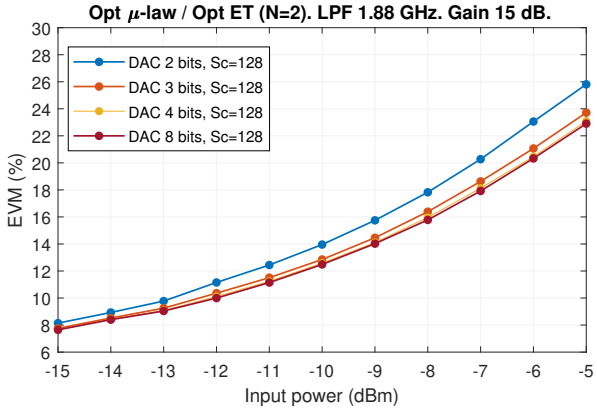

Figure 13: Influence of the DAC resolution (with 10 GHz cutoff frequency and a sampling rate of 1.88 GS/s) on the proposed ET-SOA-based CO-OFDM transmitter EVM performance, as a function of input optical power. The system operates with fixed $\{\alpha, I_{dc}, \mu, N\}$ specification resulting from PSO optimization (scenario #3). The SOA operates at a gain of 15 dB, with an input optical power of -10 dBm.

5.2 Laser wavelength shift influence

We now investigate the impact of a laser wavelength shift on the proposed μ-law/ET-SOA-based CO-OFDM transmitter while keeping the previous optimal settings calculated at the wavelength of 1540 nm with a target gain of 15 dB. As a result of the wavelength shifting, in the interval $[1480, 1560]$ nm, the SOA gain will no longer meet the initial constraint imposed for the optimization when the input optical power is changed from -18 dBm up to -4 dBm. The obtained results are reported in Fig. 14. In the first subplot (a), the EVM performance can be observed as a surface against wavelength λ and SOA input optical power. For a better perception the two following subplots (b, c) give bidimensional representations, revealing a good robustness against the wavelength variation. Over the considered range of input power, it can be seen that the EVM increase remains below 5%, compared to the original system optimized at 1540 nm. A sligth EVM improvement can possibly be obtained depending on the SOA gain which both depends on the wavelength and the SOA input power. The EVM variation against the wavelength shift tends to become more pronounced as we move towards high input optical power. What can be also observed in a last subplot, showing the SOA gain versus wavelength for various input power values, is that a relatively symmetrical behaviour occurs for the gain around 1520nm, which yields the gain peak of the amplifier. In addition, it can be seen that the gain values around this wavelength value are close to the target of 15 dB initially considered for tuning the ET sub-system.

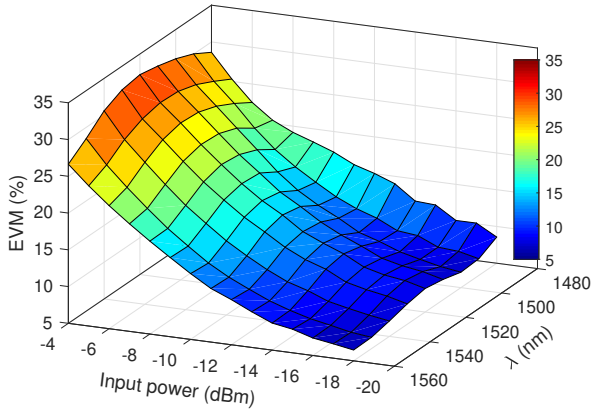

(a)

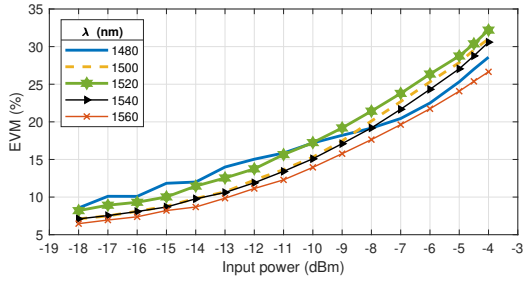

(b)

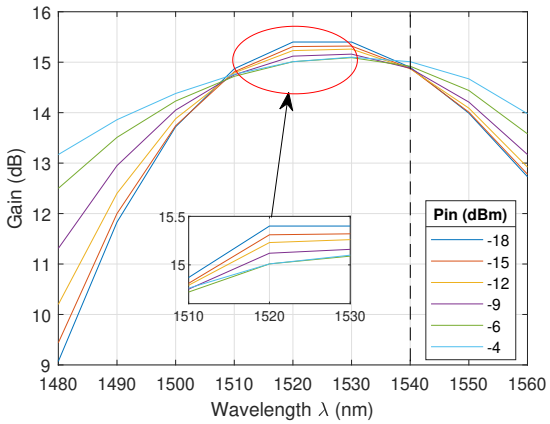

(c)

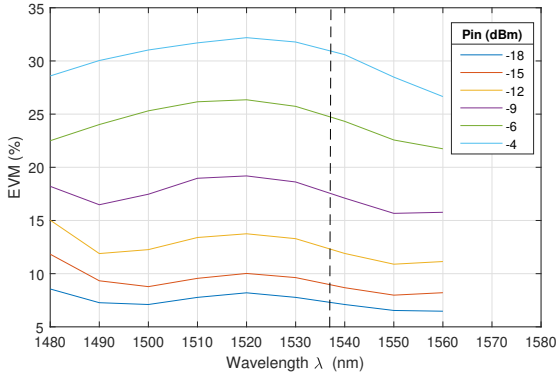

(d)

Figure 14: Wavelength shift influence on the μ-law/ET-SOA system optimized at 1540 nm. a) EVM surface against injected input power and laser wavelength λ. b) EVM as a function of input power for different laser wavelength λ. c) EVM as a function of λ for different input powers. d) SOA gain against wavelength for different input power levels.

5.3 OFDM signal bandwidth influence

A 5-GHz bandwidth may be too narrow for some coherent applications, so we conducted additional simulations at a larger bandwidth of 20 GHz for the OFDM signal to be transmitted, while keeping the same subcarrier spacing. This translates into a higher transmission speed, going up to 71 Gb/s for the 16-QAM case. As can be clearly seen in Fig. 15, the ET-SOA subsystem still offers interesting performance with no need of reoptimizing the system parameters when the electrical bandwidth is changed.

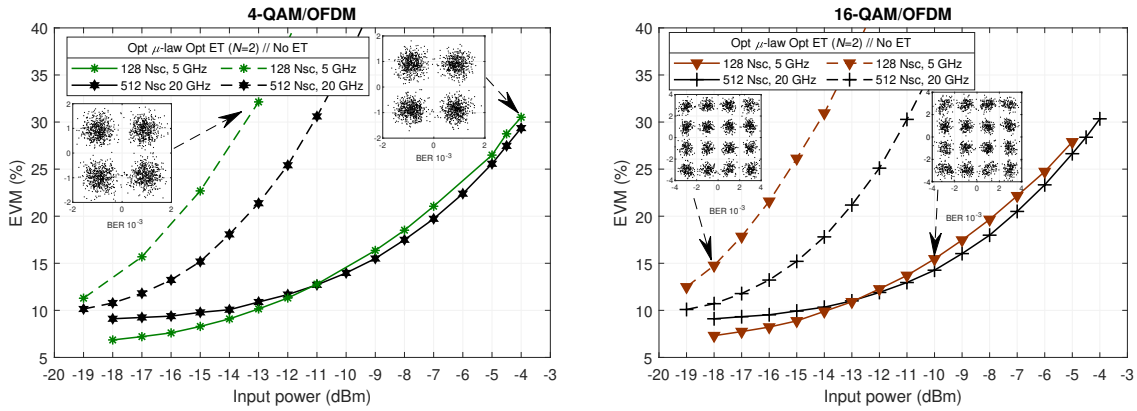

(a) (b)

Figure 15: Influence of an increased OFDM signal bandwidth (20 GHz bandwidth, the ET-SOA subsystem being optimized at 5 GHz). (a) 4-QAM transmission (b) 16-QAM transmission.

Conclusions

An envelope tracking (ET) approach has been investigated for coping with nonlinear impairments due to an SOA in a CO-OFDM transmitter. Our work is in line with the contribution of Saleh et al. [19] focusing on SOA bias current control for amplifying signals made of two tones and, to the best of our knowledge, this is the first study devoted to the optimization of the ET sub-system for multicarrier signals. Moreover, the joint use of a PAPR reduction via hard-clipping or μ-law soft-clipping is considered. Extensive simulations performed with a precise SOA model revealed that the proposed μ-law/ET scheme reduces the carrier density variation inside the SOA, which translates into a large performance increase compared to the standard system using no linearization nor PAPR reduction: up to 8 dB (resp. 7 dB) BER improvement can be achieved via the proposed scheme in the case of 4-QAM/OFDM (resp. 16-QAM/OFDM). The envelope tracking block has also shown to be robust against a wavelength shifting or some parameter changes (lowpass filter cutoff frequency, DAC characteristics or OFDM signal bandwidth) in the ET block. In particular, it was shown that even an envelope quantized with 2 bits still enables favorable performance. Hence, enveloppe tracking is an attractive solution for SOA linearization with interesting complexity/performance tradeoff and some flexibility. In this work, we adopted a classical OFDM format with cyclic prefix (CP-OFDM), but our results may be beneficial for other researchers interested in more recent multicarrier waveforms or any other non-constant envelope waveforms. The proposed approach is not either limited to use of nonlinear companding transforms and any other PAPR reduction method may be adopted for meeting the specific application constraints.

Acknowledgement

This work was partly funded by the *Consejo Nacional de Ciencia y Tecnología* (CONACYT), Mexico.

References

[1] W. Shieh, I.B. Djordjevic, OFDM for Optical Communications, Elsevier/Academic Press, 2009.

[2] J. Zhao, "DFT-based offset-QAM OFDM for optical communications", *Optics express*, 22 (1), pp. 1114-1126, 2014.

[3] E. Agrell, et al., "Roadmap of optical communications," *Journal of Optics*, vol. 18, no. 6, pp. 1- 40, 2016.

[4] Y. Rahmatallah and S. Mohan, "Peak-to-average power ratio reduction in OFDM systems: a survey and taxonomy," *IEEE Commun. Surveys Tuts.*, vol. 15, no. 4, pp. 1567-1592, Fourth Quarter 2013.

[5] A. Napoli et al., "Digital pre-compensation techniques enabling high-capacity bandwidth variable transponders", *Optics Commun.*, vol. 409, 15, pp. 52-65, 2018.

[6] S. Amiralizadeh, A. T. Nguyen, L. A. Rusch, "Modeling and compensation of transmitter nonlinearity in coherent optical OFDM", *Optics express*, 23(20), 2015.

[7] A. Amari, O. A. Dobre, R. Venkatesan, O. S. S. Kumar, P. Ciblat, and Y. Jaouën, "A survey on fiber nonlinearity compensation for 400 Gb/s and beyond optical communication systems," *IEEE Commun. Surveys Tuts.*, vol. 19, no. 4, pp. 3097–3113, 4th Quart., 2017.

[8] R. Dar and P. J. Winzer, "Nonlinear interference mitigation: methods and potential gain," *J. Lightwave Technol.*, vol. 35, no. 4, pp. 903–930, 2017.

[9] H. Khaleghi, P. Morel, A. Sharaiha, T. Rampone, "Experimental validation of numerical simulations and performance analysis of a coherent optical-OFDM transmission system employing a semiconductor optical amplifier," *J. Lightw. Technol.*, vol. 31, no. 1, pp. 161-170, Jan. 1, 2013.

[10] J. Renaudier, A. Ghazisaeidi, "Scaling Capacity Growth of Fiber-Optic Transmission Systems Using 100 + nm Ultra-Wideband Semiconductor Optical Amplifiers", *J. Lightw. Technol.*, vol. 37, no. 8, pp. 1831-1838, 2019.

[11] S. Koenig, R. Bonk, H. Schmuck, W. Poehlmann, T. Pfeiffer, C. Koos, W. Freude, J. Leuthold, "Amplification of advanced modulation formats with a semiconductor optical amplifier cascade", *Opt. Express*, 22, pp. 17854–17871, 2014.

[12] D. F. Bendimerad, Y. Frignac, "Numerical investigation of SOA nonlinear impairments for coherent transmission systems based on SOA amplification", *IEEE/OSA J. Lightwave Technol.*, 35 (24), pp. 5286-5295, 2017.

[13] X. Li and G. Li, "Joint fiber and SOA compensation using digital backward propagation," *IEEE Photon. J.*, vol. 2, no. 5, pp. 753–758, Oct. 2010.

[14] A. Ghazisaeidi and L. Rusch, "On the efficiency of digital back-propagation for mitigating SOA-induced nonlinear impairments," J. Lightwave Technol., 29 (21), 3331–3339, 2011.

[15] S. Lange et al., "A Low -complexity Digital Pre-compensation of SOA Induced Phase Distortion in Coherent QAM Transmissions," Proc. OFC/NFOEC2013, OTh3C.7, 2013.

[16] Ș. Bejan et al., "A Joint Linearization/Companding Approach for Improving a CO-OFDM Transmitter," *IEEE Photonics Technology Letters*, vol. 27, no. 20, pp. 2162–2165, Oct. 2015.

[17] F. Tabatabai and H. S. Al-Raweshidy, "Feedforward linearization technique for reducing nonlinearity in semiconductor optical amplifier," *J. Lightw. Technol.*, vol. 25, no. 9, pp. 2667–2674, Sep. 2007.

[18] L. F. Tiemeijer, G. N. van den Hoven, P. J. A. Thijs, T. van Dongen, J. J. M. Binsma, and E. J. Jansen, "1310-nm DBR-type MQW gain-clamped semiconductor optical amplifiers with AM-CATV-grade linearity," *IEEE Photon Technol. Lett.*, vol. 8, pp. 1453–1455, 1996.

[19] A. A.M. Saleh, R. M. Jopson, and T. E. Darcie," Compensation of nonlinearity in semiconductor optical amplifiers," *Electron. Lett.*, vol. 24, pp. 950-952, July 1988.

[20] W. P. Ng, A. A. E. Aziz, Z. Ghassemlooy, M. H. Aly, and R. Ngah, "Optimised non-uniform biasing technique for a highspeed optical router to achieve uniform semiconductor optical amplifier gain," *IET Communications*, vol. 6, no. 5, pp. 484–491, Mar. 2012.

[21] S O'Duill, P. Landais, and L. P. Barry : Estimation of the performance improvement of pre -amplified PAM4 systems when using multi -section semiconductor optical amplifiers, Applied Sciences , vol. 7, no. 9, p . 90 8, Sep. 2017.

[22] T. Akiyama et al., "Quantum-Dot Semiconductor Optical Amplifiers," *Proc. IEEE*, 95 (9), pp. 1757-1766 (2007).

[23] J. C. Ortiz-Cornejo, S. Bejan, S. Azou, J. A. Pardiñas-Mir and P. Morel, "On envelope-tracking for SOA amplification of multicarrier signals," 2017 IEEE International Symposium on Circuits and Systems (ISCAS), Baltimore, MD, 2017, pp. 1-4.

[24] J. C. Ortiz-Cornejo, S. Azou, J. A. Pardiñas-Mir and P. Morel, "An Improved Envelope Tracking SOA Amplifier for CO-OFDM Transmission by Using PSO," 2018 IEEE 10th Latin-American Conference on Communications (LATINCOM), Guadalajara, 2018, pp. 1-5.

[25] Schmogrow, R. et al., "Error vector magnitude as a performance measure for advanced modulation formats", *IEEE Photon. Technol. Lett.* 24, 61–63 (2012); erratum 24, 2198 (2012).

[26] M. Fujiwara and R. Koma, "Long-Reach and High-Splitting-Ratio WDM/TDM-PON Systems Using Burst-Mode Automatic Gain Controlled SOAs", IEEE J. Lightwave Technol., vol. 34, No. 3, 2016.

[27] M. Dalla Santa, C. Antony, G. Talli, and P. D. Townsend, Variable Gain SOA Pre-Amplifier for Optical Equalization of a 25Gb/s Burst-Mode PON Upstream with 10G Optics, Optical Fiber Communication Conference, San Diego, 2019.

[28] F. Wang, A. Yang, D. Kimball, L. Larson, and P. Asbeck, "Design of wide-bandwidth envelope-tracking power amplifiers for OFDM applications," *IEEE Trans. Microw. Theory Tech.*, vol. 53, no. 4, pp. 1244–1255, Apr. 2005.

[29] Z. Wang, "Demystifying envelope tracking: Use for high-efficiency power amplifiers for 4G and beyond," *IEEE Microwave Mag.*, vol. 16, no. 3, pp. 106–129, 2015.

[30] A. Sahin, I. Guvenc, and H. Arslan, "A survey on multicarrier com- munications: Prototype filters, lattice structures, and implementation aspects," IEEE Commun. Surveys Tuts., vol. 16, no. 3, pp. 1312–1338, 3rd Quart., 2014.

[31] M. J. Connelly, Semiconductor Optical Amplifiers . Boston, MA:Kluwer, 2002.

[32] C. Diouf, M. Younes, A. Noaja, S. Azou, M. Telescu, P. Morel, and N. Tanguy, "Robustness analysis of a parallel two-box digital polynomial predistorter for an SOA-based CO-OFDM system", *Opt. Commun.*, vol. 402, pp. 442-452, nov 2017.

[33] X. Wang, T. Yjhung, and C. Ng, "Reduction of peak-to.average power ratio of OFDM system using a companding technique," IEEE Trans. Bradcasting, vol. 45, no. 3, pp. 303-307, Sept. 1999.

[34] P. Morel and A. Sharaiha, "Wideband time-domain transfer matrix model equivalent circuit for short pulse propagation in semiconductor optical amplifiers," IEEE J. Quantum Electron., vol. 45, no. 2, pp. 103–116, 2009.

[35] C. Bohémond, P. Morel, A. Sharaiha, T. Rampone, and B. Pucel, "Experimental and simulation analysis of the third-order input interception point in an all-optical RF mixer based on a semiconductor optical amplifier," IEEE J. Lightwave Technol., vol. 29, no. 1, pp. 91–96, 2011.

[36] M. Hamze, "Study of different SOA structures impact on the transmission of IMDD OOFDM signals", PhD thesis, Université de Bretagne occidentale, Brest, France, 2015 (available at: https://tel.archives-ouvertes.fr/tel-02169590/document).

[37] L. M. Rios and N. V. Sahinidis, "Derivative-free optimization: a review of algorithms and comparison of software implementations," *Journal of Global Optimization*, 56(3):1247–1293, 2013.

[38] J. Kennedy, and R. Eberhart. "Particle Swarm Optimization." Proceedings of the IEEE International Conference on Neural Networks. Perth, Australia, 1995, pp. 1942–1945.